



Share Your Innovations through JACS Directory

# Journal of Nanoscience and Technology

Visit Journal at <http://www.jacsdirectory.com/jnst>

## Study on Photo-Catalytic and Antimicrobial Activity of Green Synthesized TiO<sub>2</sub> Nanoparticles Coated Vitrified Tiles

M. Sivaraj<sup>1</sup>, Swathi Sudhakar<sup>2</sup>, M. Arivanandhan<sup>1</sup>, S. Ganesan<sup>3</sup>, R. Jayavel<sup>1,\*</sup><sup>1</sup>Centre for Nanoscience and Technology, Anna University, Chennai – 600 025, Tamilnadu, India.<sup>2</sup>Department of Biotechnology, Anna University, Chennai – 600 025, Tamilnadu, India.<sup>3</sup>Department of Medical Physics, Anna University, Chennai – 600 025, Tamilnadu, India.

### ARTICLE DETAILS

#### Article history:

Received 27 June 2019

Accepted 21 August 2019

Available online 14 September 2019

#### Keywords:

Titanium Dioxide

Nanoplates

Photocatalytic Activity

### ABSTRACT

In the current study, a facile and eco-friendly method has been developed for the synthesis of titanium dioxide nanoparticles from titanium isopropoxide solution using *Datura metel* (Vellai Umathai) leaves and orange peel extract. Silver nanoparticles (60 nm) and silver nanoplates (130 nm) have been synthesized and characterized using UV-visible spectroscopy, X-ray diffractometer (XRD), atomic force microscopy (AFM) and scanning electron microscopy (SEM). The silver nanoparticles are doped with TiO<sub>2</sub> nanoparticles. The photocatalytic activity of Ag nanoparticles and nanoplates doped TiO<sub>2</sub> nanoparticles coated on vitrified tiles was investigated, wherein, degradation of methylene blue, rapidly on exposure to sunlight was observed. Analysis of the antimicrobial activity measured using colony forming units showed a 4-log reduction in the growth of the Gram-negative bacteria and a 5-log reduction in the growth of the Gram-positive bacteria.

### 1. Introduction

Biological synthesis of nanoparticles by plant extracts are at present gaining importance towards development of ecofriendly nanoparticle synthesis particularly for biomedical applications. Several plants including *Alfalfa*, *Aloe Vera*, *Cinnamum camphorra*, *Emblca officianalis*, *Carica papaya*, *Parthenium hysterophorus*, *Diopyros kaki*, *Eucalyptus hybrid*, *Hibiscus rosasinensis*, *Capsicum annum*, *Cissus quadrangularis*, *Pelargonium graveolens*, *Medicago sativa*, Lemongrass, *Capsicum annum*, *Ocimum sanctum* and tamarind have been used in the efficient and rapid synthesis of silver and gold nanoparticles. The three chief parameters towards synthesis of ecofriendly and green chemistry nanoparticle synthesis, are the choice of solvent medium, the reducing agent and the Non-toxic material used for the stabilization of nanoparticles [1,2]. Among the various biosynthetic approaches, the use of plant extracts has numerous advantages including easy availability, safety of handling and the presence of various metabolites. Titanium dioxide nanoparticles (TiO<sub>2</sub> NPs), are amongst the most important material for cosmetic, pharmaceutical [3], skin care products, essentially towards protection of skin from UV rays, providing opacity to products such as paints, plastics, papers, inks, food colorants and toothpastes [4]. The titania nanoparticles also possess interesting optical, dielectric, antimicrobial, chemical stability and catalytic properties leading to its industrial applications as pigments, fillers, catalyst supports and as photocatalysts [5]. A growing concern recently is the development of increased microbial resistance to antibiotics and the development of resistant strains for which these nanoparticles can be investigated.

Among the major applications of the TiO<sub>2</sub> nanoparticles, are the degradation of chlorinated compounds like 2-chlorophenol, 2,4-dichlorophenol and 2,4,6-trichlorophenol which are used as intermediates in the making of insecticides, herbicides, preservatives etc., which cause severe environmental pollution due to their mutagenicity and carcinogenicity [6,7]. Nanoparticulate TiO<sub>2</sub> as antibacterial coatings and wastewater disinfectants have been reported [8]. When silver is doped onto titania, it is deposited on the surface of the titania nanoparticles and not into the lattice structure of the photocatalyst. In this study, the green synthesized TiO<sub>2</sub> coated on vitrified tiles were evaluated for its

photocatalytic and antimicrobial activity. The photocatalytic activity of TiO<sub>2</sub> coated surfaces was evaluated by measuring the degradation rate of methylene blue (MB) under UV and sunlight. The antibacterial activity was evaluated using the Gram-Negative *Escherichia coli* (*E. coli*) and Gram-Positive *Lactobacillus plantarum* bacterial strains. The obtained results indicate that TiO<sub>2</sub>-coated surfaces show strong antibacterial activity suitable for industrial applications.

### 2. Experimental Methods

#### 2.1 Materials

Leaves of *Datura metel* were collected from Taramani, Chennai. Fruit extracts were collected without any impurities. Titanium tetra-isopropoxide was purchased from Avra Synthesis Pvt. Ltd, Chennai, India.

#### 2.2 Synthesis of TiO<sub>2</sub> Nanoparticles

Freshly collected leaves of *Datura metel* (10 g) were used to prepare the aqueous leaf extract, 50 g orange peel were boiled with 150 mL distilled water for 1 hour to prepare the orange peel extract, and both were stored for nanoparticle synthesis. 15 mL of solution containing 5 mL of titanium tetra-isopropoxide (TTIP) and 15 mL isopropanol were made to react with 100 mL water. To this reaction mixture 2 mL aqueous leaf extract of *Datura metel* (Vellai Umathai) was added and the pH was adjusted to 4.5 using orange peel extract. The reaction mixture was subjected to continuous stirring at 60 °C for 4 hours. There was a colour change to yellowish brown. The precipitate was collected by centrifugation and washed with distilled water, and then heated at 90 °C on a hot plate to collect the dried powder which was brown in colour.

#### 2.2.1 Synthesis of Silver Nanoparticles (Ag-NPs)

Briefly, 2 g glucose and 1 g PVP were dissolved in 40 g water and heated to 90 °C. Then 0.5 g AgNO<sub>3</sub> dissolved in 1 mL water was added. The dispersion was kept at 90 °C for 1 h and then let to cool to room temperature. The particles were collected by ultracentrifugation (29,400 g; 30 min), redispersed in pure water and collected again by ultracentrifugation leading to the removal of NO<sub>3</sub><sup>-</sup>, excess glucose and its oxidation products, excess PVP, and excess Ag<sup>+</sup>.

\*Corresponding Author: rjvel@annauniv.edu (R. Jayavel)

### 2.2.2 Synthesis of Silver Nanoplates (Ag-NPLs)

The procedure for the synthesis of silver seed hydrosol is as follows: 0.5 mL of 1.0 M  $\text{AgNO}_3$  solution and 2 mL of 4 M PVP solution were added to 17.5 mL distilled water under ice cold condition for 15 min. Then 0.3 mL of ice cold aqueous  $\text{NaBH}_4$  solution was added all at once with vigorous stirring and the stirring was continued for 45 sec. The resulting mixture was heated at 75–80 °C for 10 min to decompose excess  $\text{NaBH}_4$  present in the solution. The growth solution containing aqueous solution of 0.5 mL  $\text{AgNO}_3$ , 10 mL PVP and 0.2 mL of trisodium citrate solution were prepared in a 25 mL conical flask. Next, different volumes of seed solution were added to this growth solution under stirring for 10 min for good mixing. These solutions were then stored in the darkroom at Room temperature for 24 h.

### 2.2.3 Coating of Doped $\text{TiO}_2$ Nanoparticles on Tiles

The as-synthesized  $\text{TiO}_2$  nanoparticles were mixed with 2 mL of solution containing silver nanoparticle and nanoplates. The coating technique was adapted from the experimental guidance of Zan et al. [9]. Briefly, 2 wt.%  $\text{TiO}_2$  was mixed with aqueous solution of polyvinyl alcohol, and sonicated using ultrasound to form a poly-disperse suspension. Vitrified tiles were cut in 30 cm x 22 cm (for measurement of photocatalytic activity) and 2 cm x 2 cm (for antimicrobial activity) dimensions and were sterilized by autoclaving, wiping with alcohol and were subjected to UV exposure for 30 minutes. This was followed by a single Dip-coating procedure and the coated tiles were air-dried for 24 hours, followed by calcination at 800 °C for 1 hour. Thus, the coated tiles were used for further studies.

*E. coli* (Gram negative) and *Lactobacillus plantarum* (Gram positive) were used to assess the antibacterial potential of the green synthesized  $\text{TiO}_2$  nanoparticles. Towards this the  $\text{TiO}_2$  nanoparticle coated vitrified tiles and the uncoated tiles were covered with sterile aluminium foil and parafilm on all other sides except the smooth surface, and were sterilized under UV light for 30 minutes. The bacterial cell viability assay was performed by suspending 100  $\mu\text{L}$  per mL of 0.5 Mc Farland constant bacterial culture on 1 mL nutrient broth which was layered on the Tiles and kept under sunlight for 4 hours, and then incubated at 37 °C for 12 hours which was followed by plating on to agar plates.

## 3. Results and Discussion

### 3.1 UV-Visible Spectroscopy

The green synthesized  $\text{TiO}_2$  nanoparticles were analyzed using UV-visible optical spectroscopy. The absorption spectrum shows the characteristic peak of  $\text{TiO}_2$  at 371 nm (Fig. 1). The band gap was calculated by fitting the data using the equation  $\alpha h\nu = E_d(h\nu - E_g)$ , where,  $h\nu$  = photon energy,  $\alpha$  = energy the absorption coefficient,  $E_d$  = absorption edge width parameter,  $E_g$  = band gap and it was found to be 3.34 eV.

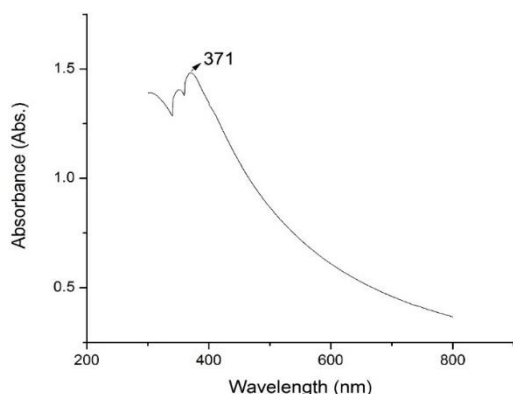


Fig. 1 UV-visible spectrum of the green synthesized  $\text{TiO}_2$  nanoparticles

### 3.2 X-Ray Diffraction Analysis

The XRD pattern reflects the shape of the wave functions of the electronic states of the Ti-O-Ti-O chain on the  $\text{TiO}_2/\text{H}_2\text{O}$  interface. XRD analysis showed three distinct diffraction peaks at 53.2°, 61.8°, 66.5° which is indexed for the planes (101), (004), (200), respectively of the cubic face centered titanium dioxide. There was a change in the crystalline structure of the nanoparticles changing from rutile before heating (Fig. 2a) to anatase after heating (Fig. 2b) [10]. The absence of identified peaks after heating confirms the crystallinity and higher purity of the synthesized nanoparticles. The average crystallite size of the nanoparticles was calculated using the Scherrer's formula,  $D = k\lambda / \beta \cos\theta$ , where D (nm) is <https://doi.org/10.30799/jnst.275.19050504>

the average crystallite size perpendicular to the reflecting planes, k is the constant which equals to 0.91,  $\lambda$  is the X-ray wavelength;  $\beta$  is the full-width at half maximum (FWHM) and  $\theta$  is the diffraction angle. The average crystallite sizes of the synthesized nanoparticles were calculated to be 80 nm before heating (Fig. 2a) and 20 nm after heating (Fig. 2b).

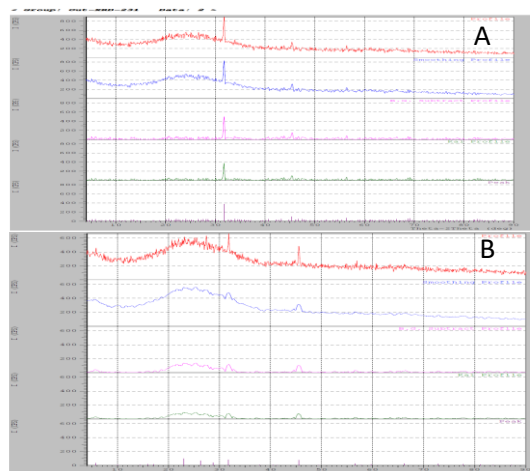


Fig. 2 XRD for synthesized  $\text{TiO}_2$  nanoparticles a) Before heating and b) After heating

### 3.3 FESEM Analysis of Green Synthesized $\text{TiO}_2$ Coated Vitrified Tiles

FESEM images of the synthesized nanoparticles were measured and topographically analyzed. They were observed to be morphologically smooth and spherical with a size of 40 nm (Fig. 3).

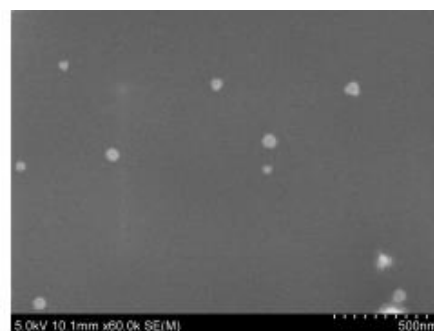


Fig. 3 FESEM image of the synthesized  $\text{TiO}_2$  nanoparticles

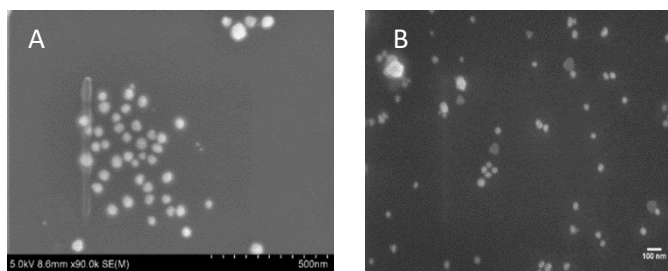
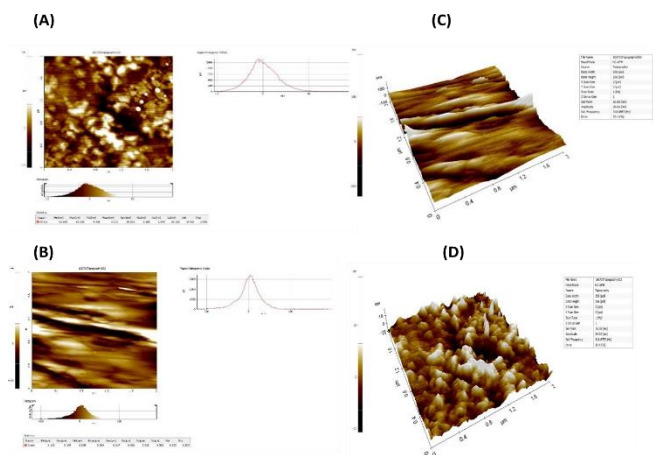


Fig. 4 FESEM images of synthesized  $\text{TiO}_2$  nanoparticles coated in tile a) Before calcination and b) after calcination

The FESEM images of the synthesized  $\text{TiO}_2$  nanoparticles coated on vitrified tiles before and after calcination are shown in Fig. 4. The green synthesized  $\text{TiO}_2$  nanoparticles coated on vitrified tiles show that the synthesized nanoparticles are highly mono dispersed particles and spherical shaped with particle size of 80–100 nm before calcination which reduced to around 15–20 nm after calcination in comparison to the size of the nanoparticle of 40 nm, which is in line with the results from XRD, confirming the role of *Datura metel* extract to change the size and morphology of the synthesized  $\text{TiO}_2$  nanoparticles.

### 3.4 Surface Analysis of The Green Synthesized $\text{TiO}_2$ Coated Tiles

Figs. 5a-d show the surface topography and roughness of the  $\text{TiO}_2$  nanoparticle coated tiles before and after heat treatment. As can be seen from the AFM images, the surface roughness of the  $\text{TiO}_2$  coated tiles have drastically decreased after heat treatment. The Fig. 5a shows surface topography of the tiles coated with  $\text{TiO}_2$  before heat treatment which shows high surface roughness, whereas the surface of the tiles is relatively smooth after heat treatment as can be seen from the Fig. 5b.



**Fig. 5** Atomic force microscopy images of  $\text{TiO}_2$  coated tiles a) roughness 2-D plot of  $\text{TiO}_2$  coated tile before heating, b) roughness 2-D plot of  $\text{TiO}_2$  coated tile after heating, c) 3-D plot of  $\text{TiO}_2$  coated tile before heating and d) 3-D plot of  $\text{TiO}_2$  coated tile after heating

### 3.5 Photocatalytic Degradation

#### 3.5.1 Optimization of the Concentration of Ag-NPs and Ag-NPLs as Dopants of the Green Synthesized $\text{TiO}_2$ Nanoparticles

The optimization of the concentration of the Ag-NPs and Ag-NPLs to act as dopants of the green synthesized  $\text{TiO}_2$  nanoparticles was performed by measuring the ratio of  $C_0$  (Initial concentration of methylene blue at time = 0) and  $C$  (concentration of methylene blue at time =  $t$ ) under UV light. Plotting of  $C/C_0$  vs Time showed the optimum concentration of 1.5 mol.% for both the Ag-NPs (Fig. 6) and the Ag-NPLs (Fig. 7).

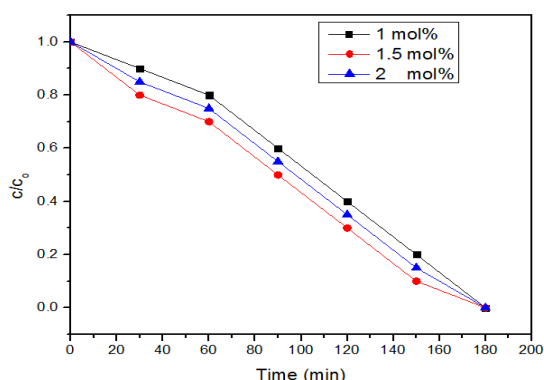


**Fig. 6** Degradation of methylene blue at 1,1.5, 2 mol.% concentrations of Ag-NPs as dopant on the green synthesized  $\text{TiO}_2$  NPs under ultraviolet rays

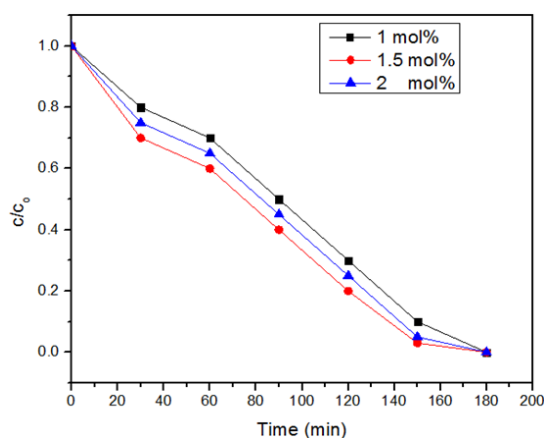


**Fig. 7** Degradation of methylene blue at 1,1.5, 2 mol.% concentrations of Ag-NPLs as dopant on the green synthesized  $\text{TiO}_2$  NPs under ultraviolet rays

#### 3.6.2 Photocatalytic Degradation of Methylene Blue under UV and Sunlight

The photocatalytic degradation of methylene blue by the green synthesized  $\text{TiO}_2$  doped with 1.5 mol.% of Ag-NPs and Ag-NPLs was studied under UV light and sunlight. Under UV radiation, an increased degradation of methylene blue was observed with the Ag-NPs and Ag-NPLs doped  $\text{TiO}_2$  in comparison to the undoped  $\text{TiO}_2$  (Fig. 8).

<https://doi.org/10.30799/jnst.275.19050504>

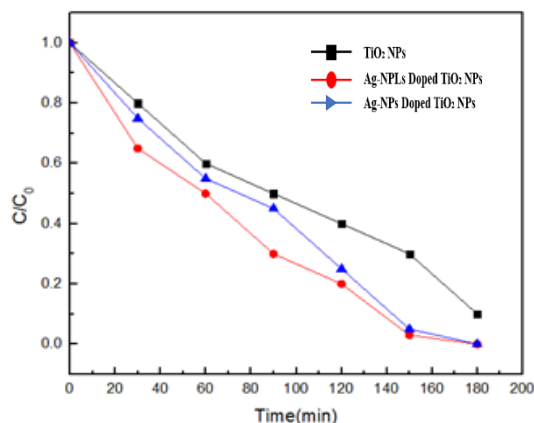


**Fig. 8** Degradation study of Methylene blue under UV radiation using 1.5 mol.% of Ag-NPs and Ag-NPLs doped  $\text{TiO}_2$  nanoparticles

A similar degradation of methylene blue by the Ag-NPs and Ag-NPLs doped green synthesized  $\text{TiO}_2$  was observed under visible light. In contrast, the undoped  $\text{TiO}_2$  showed very slight degradation of methylene blue (Fig. 9).

Interestingly, in both the studies the Ag-NPLs doped  $\text{TiO}_2$  appeared to exhibit better photocatalytic activity compared to the Ag-NPs doped  $\text{TiO}_2$ . This could be due to the larger size and the related optical properties of Ag-NPLs.

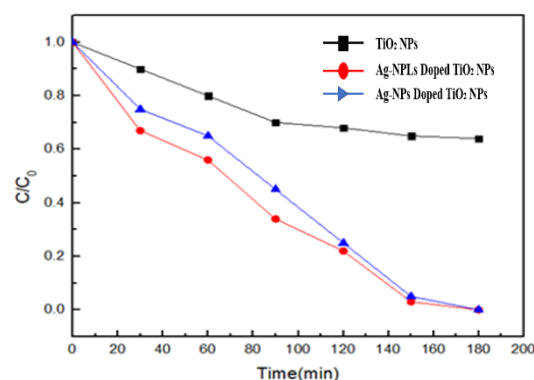


**Fig. 9** Degradation study of methylene blue under sunlight using 1.5 mol.% of Ag-NPs and Ag-NPLs doped  $\text{TiO}_2$  nanoparticles

These results confirm that the undoped and the Ag-NPs and Ag-NPLs doped  $\text{TiO}_2$  act as a photocatalyst under UV irradiation. However, under the sunlight the Ag-NPs and Ag-NPLs doped green synthesized  $\text{TiO}_2$  showed better degradation of methylene blue compared to the undoped  $\text{TiO}_2$  [11,12].

#### 3.6 Antibacterial Activity of Green Synthesized $\text{TiO}_2$ Nanoparticles

The antibacterial potential of the green synthesized  $\text{TiO}_2$  nanoparticles coated on vitrified tiles were analyzed using the Gram negative *E.Coli* and the Gram positive organism *Lactobacillus plantarum* by comparing the number of colonies formed in the control tile and the green synthesized  $\text{TiO}_2$  coated tile. The formation of colonies was studied by measuring the colony forming units (CFUs) [13,14]. For gram negative *E. coli*, the  $\text{TiO}_2$  coated tile showed 4-log reductions in the formation of the colonies in comparison to control (Figs. 10 and 11).

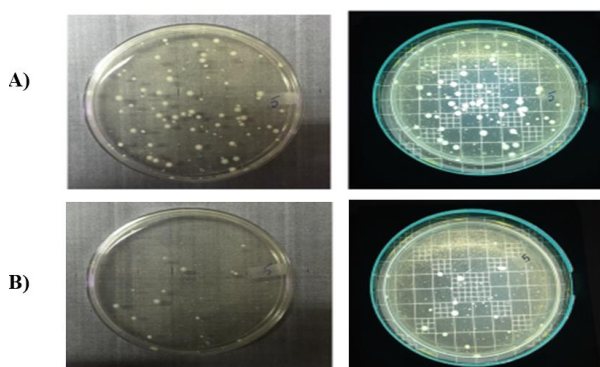


**Fig. 10** The dark and light background picture of the colonies formed at a  $10^{-5}$  dilution of both a) control and b)  $\text{TiO}_2$  treated culture

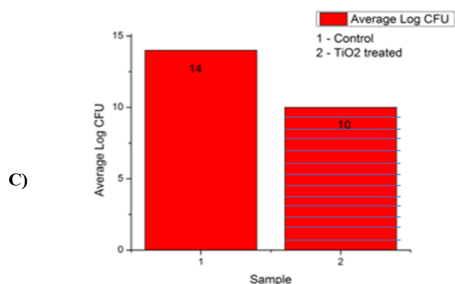


Fig. 11 Log CFU of control (*E.coli*) and TiO<sub>2</sub> treated *E.Coli*

### 3.6.2 Gram Positive- *Lactobacillus plantarum*

Analysis of the effect of the green synthesized TiO<sub>2</sub> coated tile on the formation of colonies was studied by measuring the CFUs. The TiO<sub>2</sub> coated tile showed 5-log reductions in the formation of the colonies in comparison to control (Figs. 12 and 13).

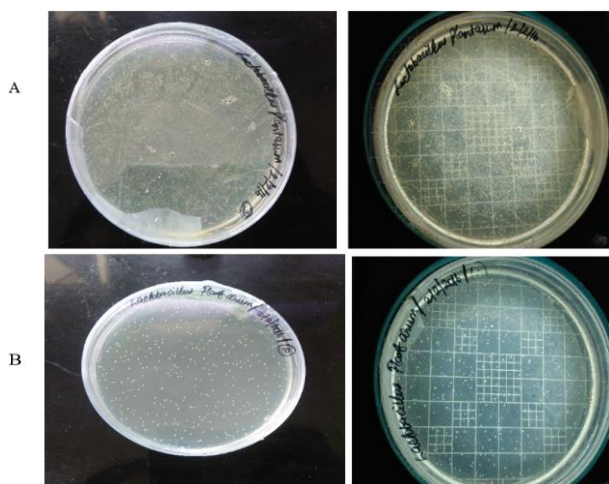


Fig. 12 The dark and light background picture of colony formed in 10<sup>-5</sup> dilution of both a) control and b) TiO<sub>2</sub> treated culture, there is a fivefold reduction in the number of colonies formed

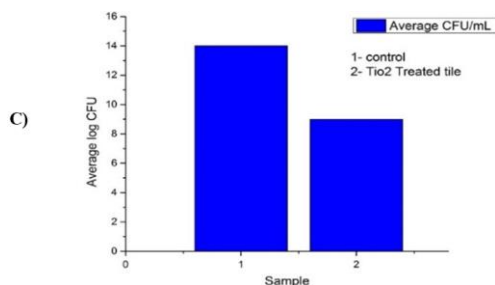


Fig. 13 Log CFU of control (*Lactobacillus plantarum*) and TiO<sub>2</sub> treated microbial cultures

## 4. Conclusion

The silver nanoparticles/nanoplates coated TiO<sub>2</sub> have been synthesized characterized for their morphology, structural and antibacterial activities. The nanoparticles were coated onto vitrified tiles and the photocatalytic activity and antibacterial effect evaluated. The photocatalytic dye degradation experiments showed a higher activity with Ag-NPs and Ag-NPLs doped TiO<sub>2</sub> nanoparticles coated tile samples. Moreover, the results obtained with TiO<sub>2</sub> coated vitrified tiles highlighted the antibacterial effect of TiO<sub>2</sub>. The results obtained indicate that the TiO<sub>2</sub>-coated surfaces show antibacterial activity highlighting that the titania could be used in the ceramic and building industry for the fabrication of coated surfaces to be placed in microbiologically sensitive environments, such as the hospital and food industry.

## References

- [1] P. Gong, H. Li, X. He, K. Wang, J. Hu, et al, Preparation and antibacterial activity of Fe<sub>3</sub>O<sub>4</sub>@ Ag nanoparticles, *Nanotechnol.* 18(28) (2007) 285604:1-7.
- [2] B. Trouiller, R. Reliene, A. Westbrook, P. Solaimani, R.H. Schiestl, Titanium dioxide nanoparticles induce DNA damage and genetic instability in vivo in mice, *Cancer Res.* 69(22) (2009) 8784-8789.
- [3] C. Gelis, S. Girard, A. Mavon, M. Delverdier, N. Paillous, P. Vicendo, Assessment of the skin photoprotective capacities of an organo-mineral broad-spectrum sunblock on two ex vivo skin models, *Photodermatol. Photoimmunol. Photomed.*, 19(5) (2003) 242-253.
- [4] R.J. Miller, S. Bennett, A.A. Keller, S. Pease, H.S. Lenihan, TiO<sub>2</sub> nanoparticles are phototoxic to marine phytoplankton, *PLoS one* 7(1) (2012) 30321:1-7.
- [5] T.A.S. Zima, L. Fialova, O. Mestek, M. Janebova, J. Crkovska, et al, Oxidative stress, metabolism of ethanol and alcohol-related diseases, *J. Biomed. Sci.* 8(1) (2001) 59-70.
- [6] S.B. Astley, Dietary antioxidants—past, present and future?, *Trends Food Sci. Tech.* 14(13) (2003)93-98.
- [7] S.J. Fox, M.H.U.T. Fazil, C. Dhand, M. Venkatesh, E.T.L. Goh, et al., Insight into membrane selectivity of linear and branched polyethylenimines and their potential as biocides for advanced wound dressings, *Acta Biomater.* 37 (2016) 155-164.
- [8] Yu. I. Golovin, Nanoindentation and mechanical properties of solids in submicrovolumes, thin near-surface layers, and films: A Review, *Phys. Solid State* 50(12) (2008) 2205-2236.
- [9] L. Zan, Z.H. Peng, Y.L. Xia, L. Huang, Novel route to prepare TiO<sub>2</sub>-coated ceramic and its photocatalytic function, *J. Mater. Sci.* 39(2) (2004) 761-763.
- [10] Babak Sadeghi, S. Farshid, M. Garmaroudi, M. Hashemi, H.R. Nezhad, et al, Comparison of the anti-bacterial activity on the nanosilver shapes: Nanoparticles, nanorods and nanoplates, *Adv. Powder Technol.* 23 (2012) 22-26.
- [11] P. Cheng, M. Zheng, Y. Jin, Q. Huang, M. Gu, Preparation and characterization of silica-doped titania photocatalyst through sol-gel method, *Mater. Lett.*, 57(20) (2003) 2989-2994.
- [12] A. Tripathy, A.M. Raichur, N. Chandrasekaran, T.C. Prathna, A. Mukherjee, Process variables in biomimetic synthesis of silver nanoparticles by aqueous extract of *Azadirachta indica* (Neem) leaves, *J. Nanopart. Res.* 12(1) (2010) 237-246.
- [13] D.C.L. Vasconcelos, E.H.M. Nunes, M. Gasparon, W.L. Vasconcelos, Infrared spectroscopy of titania sol-gel coatings on 316L stainless steel, *Mater. Sci. Appl.* 2(10) (2011) 1375-1382.
- [14] A. Krishnasamyet, M. Sundaresan, P. Velan, Rapid phytosynthesis of nano-sized titanium using leaf extract of *Azadirachta indica*, *Int. J. ChemTech Res.* 8(4) (2015) 2047-2052.